# Use of the Natural Nucleotide, GTP, is Essential for the Identification of Potent, Active-State KRAS$^{G12C}$ Inhibitors That Bind in the Switch II Pocket

**Bin Wang[1], Alok K. Sharma[2], James P. Stice[1], Brian Smith[2], Marcin Dyba[2], Devansh Singh[1], John Paul Denson[2], Dana Rabara[2], Erik Larsen[2], Yue Yang[3], Felice C. Lightstone[3], Andrew Stephen[2], Dwight V. Nissley[2], Frank McCormick[1,2], Eli Wallace[1], Anna E. Maciag[2], Pedro J. Beltran[1]**

[1]BridgeBio Pharma Inc., Palo Alto, CA; [2]Frederick National Laboratory for Cancer Research, Frederick, MD; [3]Lawrence Livermore National Laboratory, Livermore, CA

## BACKGROUND

Mutations in codon 12 of KRAS are observed in many human cancers. KRAS$^{G12C}$ mutations are found in ~15% of non-small cell lung cancers and in a low percentage of colorectal and pancreatic adenocarcinomas[1]. These activating mutations in KRAS push cellular balance towards its active, GTP-bound state that signals downstream and drives cellular transformation[2]. Recently approved inhibitors of KRAS$^{G12C}$ that bind and sequester the oncogenic protein in its inactive, GDP-bound state, have demonstrated clinical efficacy in patients with KRAS$^{G12C}$ cancers, including NSCLC, CRC and pancreatic adenocarcinoma[3-6]. However, duration of response has been shorter than expected from the potent inhibition of a driver oncogene[7,8] . This quick emergence of acquired resistance has been attributed to reactivation of MAPK signaling through multiple mechanisms, including RTK signaling and KRAS$^{G12C}$ gene amplification, resulting in increased active, GTP-bound KRAS$^{G12C}$ [9-12]. To address this unmet need, we have developed a series of dual state inhibitors and here summarize their activity against the active and inactive states of the KRAS$^{G12C}$ protein.

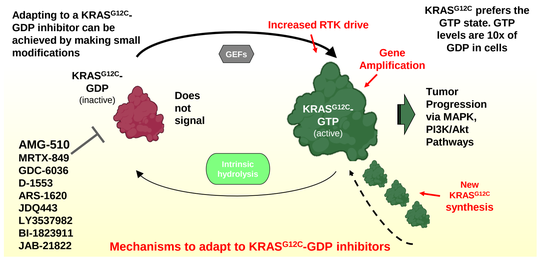


**KRAS$^{G12C}$-GDP Inhibitors Target a "Dead" Protein With No Signaling or Transforming Potential**. KRAS$^{G12C}$ GDP inhibitors rely on the conversion to active RAS to show efficacy. For inactive state (GDP) inhibitors, a number of mechanisms could result in a loss of potency, including increased RTK drive, KRAS$^{G12C}$ amplification, as well as newly synthesized KRAS$^{G12C}$ leading to reactivation of the MAPK and PI3K pathways resulting in tumor progression. Active state inhibitors may overcome these resistance mechanisms and this rationale provided the impetus for the development of our potent series

## OBJECTIVES

- Characterize the potency of a series of KRAS$^{G12C}$ inhibitors using a variety of biochemical and cell-based assays that measure GDP and GTP activity.
- Demonstrate that the GTP analog, GppNHp, versus the natural substrate GTP substantially overestimates the potency of KRAS$^{G12C}$ inhibitors in assays that measure the GTP-bound KRAS$^{G12C}$ activity.

## MATERIALS AND METHODS

- **Homogeneous Time Resolved Fluorescence (HTRF) pERK Assay:** H358 cells were seeded at 30,000 cells/well in a 96-well plate and allowed to adhere overnight. The next day, cells were treated with compound for 30min-2 hours and samples were processed with a CisBio Phospho-ERK 1/2 (Thr202/204) cellular kit, HTRF (Cat. No. 64ASPEG).
- **CellTiter-Glo 3D Viability Assay:** H358 cells were seeded 1,000 cells/well in an ultra-low attachment 3D plate.and allowed for spheroids to form for 2 days. Cells were then treated with compound for 7 days and samples were processed with a Promega CellTiter-Glo® 3D Cell Viability Assay (Cat. No. G9683).
- **Mass Spectrometry-Based Covalent Engagement Assay:** 1 µM solutions of GTP, GppNHp and GDP-loaded KRAS4b (amino acids 1-169)-G12C/C118S protein were prepared and dispensed onto plates and then 30 nL of tested compounds from 1 mM DMSO stocks were added to the appropriate wells. At 15 minutes, 2 µL of each reaction mixture was pipetted into 15 µL MALDI matrix solution deposited onto plates. The resulting solution was mixed by aspiration, centrifuged at 2000 *g* for 1 minute, and then 1.5 µL aliquots were dispensed on pre-treated MALDI target. MALDI-TOF measurements were performed on Bruker Daltonics rapifleX Tissuetyper TOF-TOF mass spectrometer using linear mode and mass range from 18.6 to 21.6 kDa. Percent modification was calculated as a ratio of peak height for protein modified by compound to sum of peak height of remaining protein plus peak height for protein modified by compound. The mean percent modifications from 17 experiments are shown.
- **PPI:** Avi-KRAS$^{G12C}$ (amino acids 2-169) GTP/GppNHp and RAF1 RBD-3xFLAG (amino acids 51-131) and HTRF reagents were mixed and dispensed onto plates and then incubated for 1 hour at room temperature with shaking. Plates were analyzed on an Envision plate reader. Data was reported as percentage of activity with DMSO as 100% and plotted and analyzed using Graph Prism 8. Representative results are shown and the mean $IC_{50}$ values from 6 experiments was calculated.
- **RAS-RAF ELISA:** MiaPaca-2 cells were seeded 280,000 cells/well and allowed to adhere overnight. Cells were treated with 1µM of compound for 5,15,30, and 60 minutes and lysate were processed using a commercially available ELISA kit (Abcam# ab134640). Briefly, lysates collected and incubated with a RAF-RAS binding domain conjugated to bottom of ELISA plate, followed by a KRAS detection ab and luciferase conjugated secondary antibody. Luciferase signal was measured on a Clariostar plate reader.
- **HeLa A59G Western: HeLa Tet-ON KRAS$^{G12C/A59G}$ Western blot:** HeLa cells were engineered to express the KRAS$^{G12C/A59G}$ under control of doxycycline-induced promoter. Cells were transduced with lentivirus and selected with 1ug/mL puromycin for several passages. Cells were plated at 1.25e6 cells in 10 cm dish into media containing 200 ng/ml doxycycline, allowed to attach for 24h, then treated for 2 hours with various doses of compound. Following treatment, cells lysates were collected and processed for Western blot using phospho-ERK (Thr202/204), total ERK, KRAS, and vinculin. All antibodies were procured from Cell Signaling Technologies.

## Figure 1: Potency Profiles of KRAS$^{G12C}$ Inhibitors

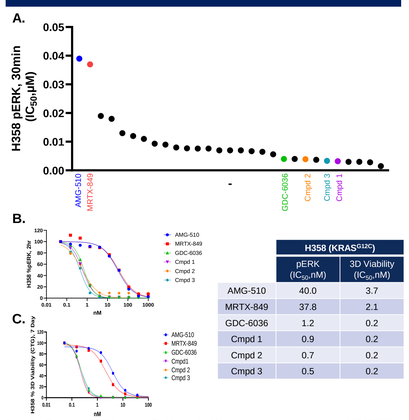


| | H358 (KRAS$^{G12C}$) | |
|---|---|---|
| | pERK ($IC_{50}$,nM) | 3D Viability ($IC_{50}$,nM) |
| AMG-510 | 40.0 | 3.7 |
| MRTX-849 | 37.8 | 2.1 |
| GDC-6036 | 1.2 | 0.2 |
| Cmpd 1 | 0.9 | 0.2 |
| Cmpd 2 | 0.7 | 0.2 |
| Cmpd 3 | 0.5 | 0.2 |

**Fig. 1: Phospho-ERK and 3D Viability $IC_{50}$s across a series of KRAS$^{G12C}$ inhibitors**. $IC_{50}$s of a series of compounds profiled at 30min (A) or at 2 hours (B) for phospho-ERK by HTRF or at day 7 for 3D viability (C). Compounds 1, 2, 3 as well as GDC-6036 show equivalent potency and are approximately 40-fold more potent on pERK and 10 to 15-fold more potent on 3D viability than AMG-510 or MRTX-849.

## Figure 2: Covalent KRAS$^{G12C}$ Labeling Reveals That the Potency of "Active State" Inhibitors can be Overestimated When Using GppNHp

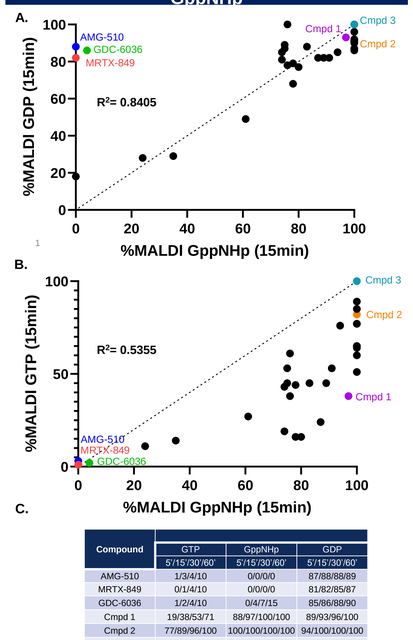


| Compound | GTP | GppNHp | GDP |
|---|---|---|---|
| | 5'/15'/30'/60' | 5'/15'/30'/60' | 5'/15'/30'/60' |
| AMG-510 | 1/3/4/10 | 0/0/0/0 | 87/88/88/89 |
| MRTX-849 | 0/1/4/10 | 0/0/0/0 | 81/82/85/87 |
| GDC-6036 | 1/2/4/10 | 0/4/7/15 | 85/86/88/90 |
| Cmpd 1 | 19/38/53/71 | 88/97/100/100 | 89/93/96/100 |
| Cmpd 2 | 77/89/96/100 | 100/100/100/100 | 94/100/100/100 |
| Cmpd 3 | 96/100/100/100 | 100/100/100/100 | 100/100/100/100 |

**Fig. 2: Correlation between covalent labeling of GppNHp vs GDP or GTP in a series of KRAS$^{G12C}$ GDP and GTP inhibitors.** A series of compounds was run on MALDI for 15 minutes and analyzed for KRAS$^{G12C}$ modification in the presence of GTP, GppNHp, or GDP and analyzed for their linear correlation. AMG-510, MRTX-849 and GDC-6036 showed no labeling in the presence of GTP or GppNHp and were removed for linear regression analysis. GppNHp displayed a stronger correlation to GDP (A) than GTP (B) on the series of compounds tested. A select number of compounds (C) are highlighted to demonstrate agreement between GppNHp and GTP (Cmpd 3>Cmpd 2) and those with large discrepancy (Cmpd 1).

## Figure 3: Covalent Labeling Findings Correlate With a PPI Assay: Only Compounds With GppNHp Activity Show Potency and GppNHp Overestimates Potency vs GTP

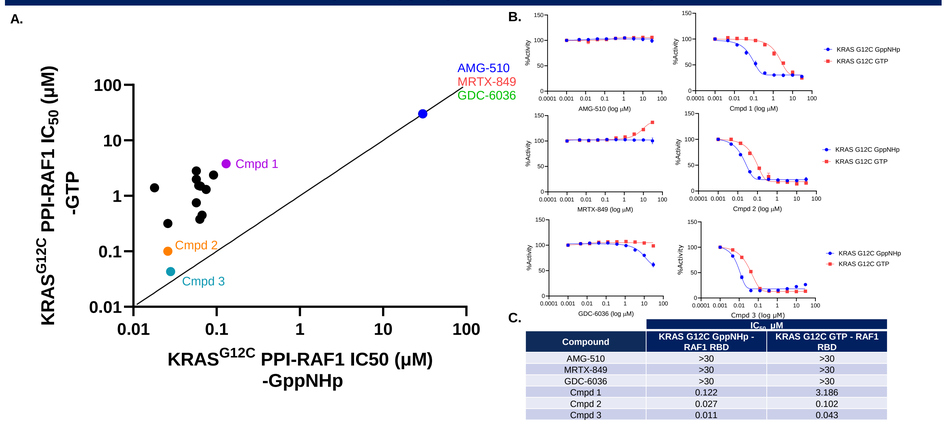


| Compound | $IC_{50}$, µM | |
|---|---|---|
| | KRAS G12C GppNHp - RAF1 RBD | KRAS G12C GTP - RAF1 RBD |
| AMG-510 | >30 | >30 |
| MRTX-849 | >30 | >30 |
| GDC-6036 | >30 | >30 |
| Cmpd 1 | 0.122 | 3.186 |
| Cmpd 2 | 0.027 | 0.102 |
| Cmpd 3 | 0.011 | 0.043 |

**Fig. 3: RAF1-KRAS$^{G12C}$ protein-protein interactions show loss of activity in presence of GTP vs. GppNHp.** Compounds were profiled for potency in the disruption of KRAS$^{G12C}$ with RAF1 by FRET. $IC_{50}$s of each compound were compared under GTP vs GppNHp conditions are plotted on the left (A) and representative curves (B) of a select number of compounds and a table (C) of their $IC_{50}$s are shown on the right. The majority of compounds demonstrated loss of potency on GTP vs. GppNHp. Similar to results seen in MALDI, Cmpd 3>Cmpd 2>Cmpd 1 in terms of correlation, whereas AMG-510, MRTX-849, and GDC-6036 had no activity in the PPI assay.

## Figure 4: Inhibition of RAS-RAF Binding Shows a Stronger Correlation Between Modification of GTP-Bound vs GppNHp-Bound KRAS

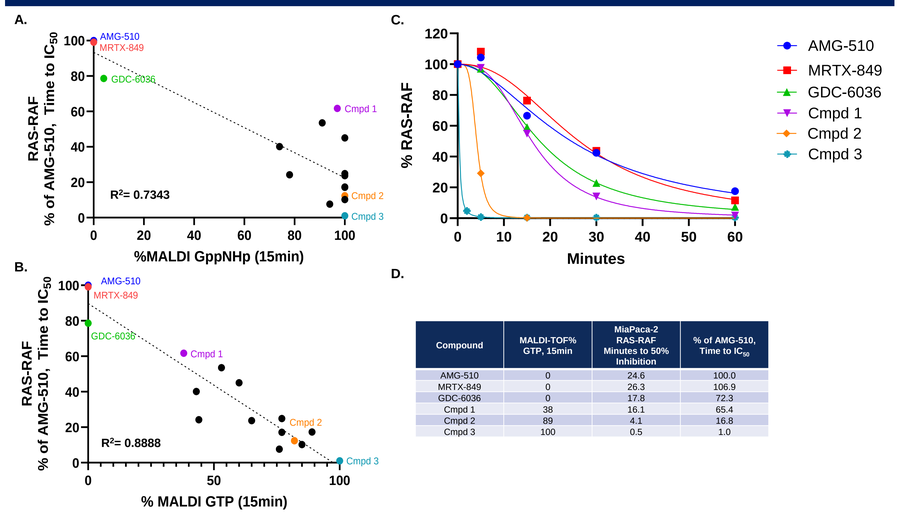


| Compound | MALDI-TOF% GTP, 15min | MiaPaca-2 RAS-RAF Minutes to 50% Inhibition | % of AMG-510, Time to $IC_{50}$ |
|---|---|---|---|
| AMG-510 | 0 | 24.6 | 100.0 |
| MRTX-849 | 0 | 26.3 | 106.9 |
| GDC-6036 | 0 | 17.8 | 72.3 |
| Cmpd 1 | 38 | 16.1 | 65.4 |
| Cmpd 2 | 89 | 4.1 | 16.8 |
| Cmpd 3 | 100 | 0.5 | 1.0 |

**Fig. 4: Cell-Based RAS-RAF ELISA disruption shows stronger correlation to MALDI GTP vs GppNHp**. The potency of various compounds on the disruption of the RAS-RAF interaction was measured in MiaPaca-2 cells using a commercially available ELISA kit. Results comparing the $IC_{50}$ from the ELISA to the MALDI labeling on GppNHp (A) vs GTP (B) are shown on the left. To the right are the representative curves (C) for a select number of compounds in the RAS-RAF ELISA along with a table (D) comparing their labeling by MALDI in the presence of GTP along with their time to inhibition in the RAS-RAF ELISA. In summary, RAS-RAF results had a stronger correlation to MALDI GTP vs GppNHp MALDI labeling and Cmpd 3 showed the fastest inhibition followed by compound 2, 1, then GDP inhibitors GDC-6036, MRTX-849, and AMG-510.

## Figure 5: In a KRAS GTP "Locked" G12C/A59G Mutant, Compounds With Higher GTP Labeling Display Greater Potency

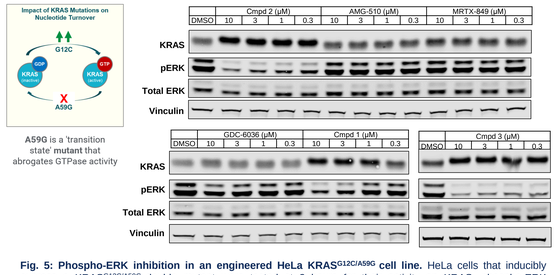


**Fig. 5: Phospho-ERK inhibition in an engineered HeLa KRAS$^{G12C/A59G}$ cell line.** HeLa cells that inducibly express a KRAS$^{G12C/A59G}$ double mutant were tested at 2 hours for their activity on KRAS, phospho-ERK (Thr202/204), total ERK and vinculin as a loading control, using 0.3 to 10µM of selected compounds. Compound 3 demonstrated the greatest inhibition on pERK followed by compound 2 and 1, whereas compounds without GTP activity (AMG-510, MRTX-849, GDC-6036) had no inhibition of phosphorylated ERK.

## RESULTS

In order to overcome active KRAS$^{G12C}$-driven resistance, we have developed direct KRAS$^{G12C}$ small molecule inhibitors that inhibit both the active, GTP-bound and inactive, GDP-bound forms of KRAS$^{G12C}$ through interactions with the switch II pocket, and independently of any other partner proteins. Mass spectrometry analysis of KRAS$^{G12C}$ covalent engagement shows complete modification of both KRAS$^{G12C}$ active, GTP-bound and inactive, GDP-bound proteins, while sotorasib (AMG-510), adagrasib (MRTX-849), and divarasib (GDC-6036) only modify the inactive, GDP-bound protein. As expected, our active state inhibitors also show potent inhibitory activity in an effector (RAF1) disruption assay where inactive, GDP-bound inhibitors demonstrate no measurable potency. Interestingly, during our work assessing the potency of these direct KRAS$^{G12C}$ inhibitors of the active state, we discovered that employing the broadly used non-hydrolyzable GTP nucleotide analog GppNHp as a surrogate for the natural nucleotide GTP results in overestimation of potency. These differences in potency between GppNHp and GTP were biologically meaningful as only compounds with strong activity against GTP-bound KRAS$^{G12C}$ were able to demonstrate cellular activity consistent with inhibition of the active, GTP-bound state which leads us to identify a series of potent dual KRAS$^{G12C}$ inhibitors.

## CONCLUSIONS

- Inhibiting the active, GTP-bound state of KRAS$^{G12C}$ is possible with switch II pocket binders.
- Using the natural, physiological nucleotide, GTP, in biochemical assays is indispensable to identify compounds with corresponding cellular activity that is differentiated from molecules that target the inactive, GDP-bound state of KRAS$^{G12C}$.

1. Nassar AH, Adib E, and Kwiatkowski DJ. Distribution of KRASG12C Somatic Mutations Across Race, Sex, and Cancer Type. N Engl J Med 2021; 384(2):185-187.
2. Moore AR, Rosenberg SC, McCormick F et al. RAS-targeted therapies: is the undruggable drugged? Nat Rev Drug Discov 2020; 19(8):553-552.
3. Ostrem JM, Peters U, Sos ML et al. KRAS (G12C) Inhibitors Allosterically Control GTP Affinity and Effector Interactions. Nature 2013; 502(7477):548-51.
4. Lito P, Solomon M, Li LS, Hansen R, Rosen N. Allele-specific inhibitors inactivate mutant KRAS G12C by a trapping mechanism. Science 2016;351(6273):604-608.
5. Canon J, Rex K, Saiki AY, et al. The clinical KRAS(G12C) inhibitor AMG 510 drives antitumour immunity. Nature 2019;575(7781):217-223.
6. Hallin J, Engstrom LD, Hargis L, et al. The KRAS(G12C) Inhibitor MRTX849 Provides Insight Toward Therapeutic Susceptibility of KRAS-Mutant Cancers in Mouse Models and Patients. Cancer Discov 2020;10(1):54-71.
7. Skoulidis F, Li BT, Dy GK, et al. Sotorasib for Lung Cancers with KRAS p.G12C Mutation. N Engl J Med 2021;384(25):2371-2381.
8. Fakih MG, Kopetz S, Kuboki Y, et al. Sotorasib for previously treated colorectal cancers with KRASG12C mutation (CodeBreaK100): a prespecified analysis of a single-arm, phase 2 trial. Lancet Oncol 2022;23(1):115-124.
9. Awad MM, Liu S, Rybkin, II, et al. Acquired Resistance to KRAS(G12C) Inhibition in Cancer. N Engl J Med 2021;384(25):2382-2393.
10. Ryan MB, Fece de la Cruz F, Phat S, et al. Vertical Pathway Inhibition Overcomes Adaptive Feedback Resistance to KRAS(G12C) Inhibition. Clin Cancer Res 2020;26(7):1633-1643.
11. Tanaka N, Lin JJ, Li C, et al. Clinical acquired resistance to KRASG12C inhibition through a novel KRAS switch-II pocket mutation and polyclonal alterations converging on RAS-MAPK reactivation. Cancer Discov 2021;11(8):1913-1922.
12. Xue JY, Zhao Y, Aronowitz J, et al. Rapid non-uniform adaptation to conformation-specific KRAS(G12C) inhibition. Nature 2020;577(7790):421-425.